



OPEN

Homozygous substitution of threonine 191 by proline in polymerase η causes Xeroderma pigmentosum variant

Roberto Ricciardiello^{1,2}, Giulia Forleo¹, Lina Cipolla¹, Geraldine van Winckel³, Caterina Marconi³, Thierry Nospikel³, Thanos D. Halazonetis⁴, Omar Zgheib³✉ & Simone Sabbioneda¹✉

DNA polymerase eta (Pol η) is the only translesion synthesis polymerase capable of error-free bypass of UV-induced cyclobutane pyrimidine dimers. A deficiency in Pol η function is associated with the human disease Xeroderma pigmentosum variant (XPV). We hereby report the case of a 60-year-old woman known for XPV and carrying a Pol η Thr191Pro variant in homozygosity. We further characterize the variant in vitro and in vivo, providing molecular evidence that the substitution abrogates polymerase activity and results in UV sensitivity through deficient damage bypass. This is the first functional molecular characterization of a missense variant of Pol η , whose reported pathogenic variants have thus far been loss of function truncation or frameshift mutations. Our work allows the upgrading of Pol η Thr191Pro from 'variant of uncertain significance' to 'likely pathogenic mutant', bearing direct impact on molecular diagnosis and genetic counseling. Furthermore, we have established a robust experimental approach that will allow a precise molecular analysis of further missense mutations possibly linked to XPV. Finally, it provides insight into critical Pol η residues that may be targeted to develop small molecule inhibitors for cancer therapeutics.

Xeroderma pigmentosum variant (XPV), an autosomal recessive disease, was first described in 1970 as having a similar phenotype to xeroderma pigmentosum (XP), however with less severe sun sensitivity, freckling, neoplastic transformation and a later onset¹. Its molecular basis also differs from that of XP, as translesion synthesis (TLS) and not nucleotide excision repair (NER) is defective in XPV. Complementation assays with HeLa cell isolates led to the identification in 1999 of DNA polymerase eta (Pol η), highly conserved in eukaryotes, and capable of restoring replication of DNA containing cyclobutane pyrimidine dimers (CPD)². Pol η , which is constitutively present at the replication fork, enables efficient thymine-thymine (TT) dimer replication. It can also bypass, albeit less efficiently, other lesions such as O6-methylguanine (O6mG), 8-oxoguanine (8-oxoG), and cisplatin-induced guanine-guanine (GG) adducts³. Pol η is the only TLS polymerase capable of error-free bypass of UV-induced CPD, and it was the first TLS polymerase associated with a human disease. The gene coding for Pol η is *POLH* and contains 11 exons located on 6p21.1-6p12.3. The importance of TLS in human health is further strengthened by recent findings showing that mutations in *REV3L*, a gene encoding for another TLS polymerase, can cause Möbius syndrome⁴ and developmental delay with hypotrophy⁵.

The mechanism behind TLS involves monoubiquitylation of the Proliferating Cell Nuclear Antigen (PCNA), promoting its interaction with Pol η and facilitating the polymerase switch⁶. The crystal structure of Pol η 's catalytic domain was first solved in *S. cerevisiae* and it provided the basis for its unique function in faithfully replicating DNA containing a CPD. This capability is linked to its wider and more open active site that can accommodate more than one unpaired nucleotide⁷. On the other hand, this specific feature makes the polymerase more prone to errors when replicating undamaged DNA.

The structure of the catalytic domain of human Pol η was solved in 2010 and it similarly features a large active site. The full protein is composed of 713-amino acids, with an N-terminal catalytic domain and a C-terminal

¹Istituto di Genetica Molecolare "Luigi Luca Cavalli-Sforza", CNR, Pavia, Italy. ²Dipartimento di Biologia e Biotecnologie "Lazzaro Spallanzani", Università degli Studi di Pavia, Pavia, Italy. ³Division of Medical Genetics, Diagnostics Department, Geneva University Hospitals, Geneva, Switzerland. ⁴Department of Molecular and Cellular Biology, University of Geneva, Geneva, Switzerland. ✉email: omar.zgheib@hcuge.ch; simone.sabbioneda@igm.cnr.it

region comprising the PCNA interacting region, a ubiquitin-binding domain (UBZ), a nuclear localization signal (NLS) and domains that bind REV1, another TLS polymerase, and POLD2, a subunit of the replicative Pol δ polymerase^{8–10}. The first 500 residues of Pol η constitute the catalytic domain, whose structure, spanning residues 1–432, is composed of a palm (1–18, 88–239), finger (16–87), thumb (240–306) and little finger (307–432) domains¹⁰.

A search of the main public archives that report evidence-based relationships among human variations and phenotypes, namely Human Gene Mutation Database (HGMD), Leiden Open Variation Database (LOVD), and NCBI's ClinVar, shows that all reported pathogenic or likely pathogenic Pol η variants are loss of function truncation or frameshift mutations, mainly in the catalytic domain. To date, no missense variant has been reported as being pathogenic or likely pathogenic, owing to the lack of evidence-based in vitro or in vivo functional studies adhering to the American College of Medical Genetics and Genomics (ACMG) guidelines for variant interpretation¹¹.

A Thr191Pro variant was recently identified in Brazilian XPV patients and it was associated with skin tumors, namely squamous cell carcinoma (SCC). This variant, alongside others identified in the same study, was reported as of uncertain significance (VUS) due to the lack of functional data¹².

Here we report the case of a 60-year-old woman carrying the Thr191Pro variant in homozygosity. We characterize Pol η carrying the amino acid substitution in vitro and in vivo, providing molecular evidence that the substitution abrogates polymerase activity and results in UV sensitivity through deficient damage bypass.

Results

The patient, who was referred to us for genetic counseling and testing, was known for XPV since her late teens. She presented initial freckling at age four and a first nose lesion at age 14. Recurrence after multiple excisions prompted a skin graft on her nose at age 24, at which time she started follow-ups at our university hospital. She later developed multiple squamous and basal cell carcinomas (BCC), as well as melanomas, mostly on the face and limbs. She also presented right renal atrophy and a small head circumference (52 cm, < P3) (Fig. 1A–C). There were no neurological symptoms and ophthalmological assessment was normal.

Family history showed that her parents were first-degree cousins of Portuguese descent. She had six siblings, including a brother and sister who passed away in an accident at age 36 and from renal disease at age 26, respectively. Her four other sisters, one of whom was described as having freckles and a normal skin biopsy, were in good health. None of her siblings was known for skin cancer (Fig. 2).

In this setting of an inbred patient with XPV, we highly suspected a homozygous mutation in *POLH* and carried out targeted exome sequencing. We found no variants in a gene panel of XP, trichothiodystrophy, or Cockayne syndrome, except for one, at the homozygous state, in *POLH*: NM_006502:exon5:c.571A>C:p.Thr191Pro. In the absence of functional data, the variant was classified as of uncertain significance (VUS).

Our search of the literature found that it was reported for the first time in 2020 in XPV patients and indeed classified then as VUS¹². Only the nucleotide substitution (c.571A>C) was reported in the body of the article, with the supplementary section indicating the resulting Thr191Pro substitution. Its predicted functional impact was not described, and no functional assays were performed.

Thr191 is located away from the nucleotide binding site, but in the midst of an alpha-helix in the palm domain, its hydroxyl sidechain making close contact with the sidechain nitrogen of Trp174, located in an opposite alpha-helix, and the backbone carboxyl of Asp187, four residues upstream. Thr191's backbone carboxyl makes contact with the backbone amide N–H of Ala194 and Val195. Proline substitution would not only result in loss of these stabilizing interactions, but also introduce a kink in the alpha-helix. This is expected to induce a conformational change that may disturb the openness of the active site, critical to Pol η function¹⁰ (Fig. 3).

We therefore sought to characterize this variant by performing a primer extension assay in vitro and by evaluating S-phase stalling and survival in vivo after UV irradiation in stable cell lines expressing wild-type Pol η or the Thr191Pro variant. To assess the catalytic properties of the Thr191Pro variant, the substitution was inserted in a Pol η coding expression vector that was subsequently used for in vitro coupled transcription and translation

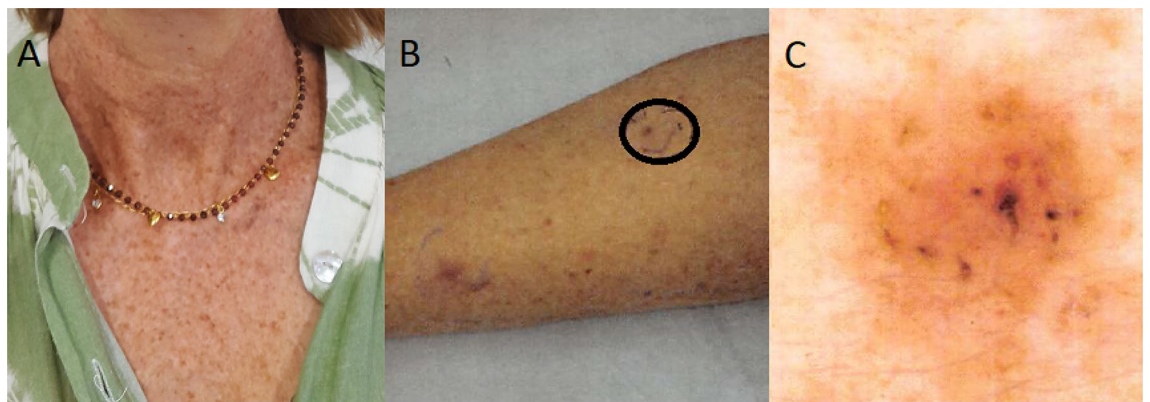


Figure 1. (A) Patient photographs showing freckles on neck and torso; (B) Patient's leg with a close-up view (C) of a superficial basal cell carcinoma before excision.

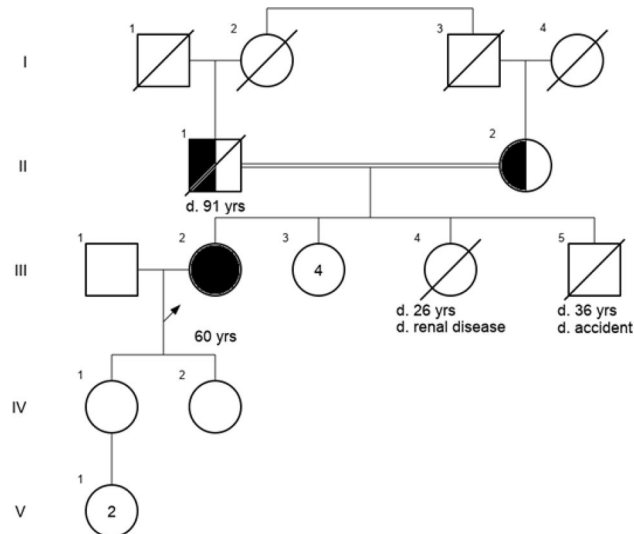


Figure 2. Patient's pedigree.

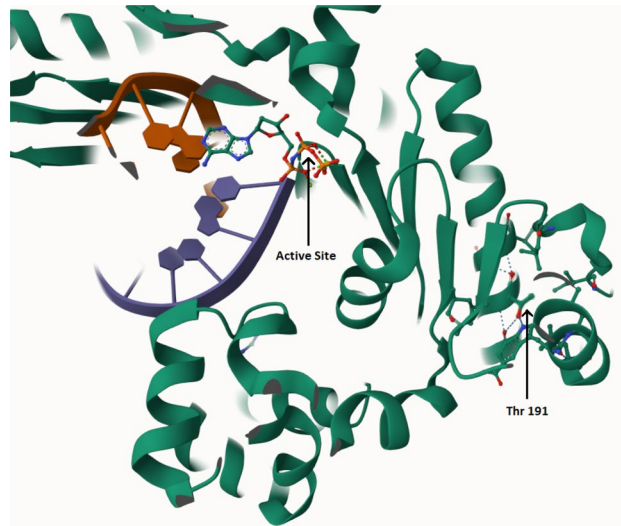


Figure 3. Mol* Viewer three-dimensional structure of Pol η showing the catalytic domain with the DNA double strand and an incoming nucleotide in the active site. Thr191 is shown with stabilizing intra- and inter-helical interactions (see text for details).

in a reticulocyte extract (TnT system, Promega). The variant, along a wild-type (WT) construct and the corresponding empty vector control (EV), was then analyzed in an *in vitro* primer extension assay using as a 16 bp primer annealed to a 30 bp template, either undamaged or containing a thymidine CPD located in position +1 relative to the end of the primer (Fig. 4A,B). In the case of the undamaged template, distributive elongation of the primer was observed in the *in vitro* system, as the reticulocyte extract itself was partially competent for DNA replication (Fig. 4A, lane 2). As previously shown¹³, Pol η WT completely elongated the primer in a highly processive manner (Fig. 4A, lane 3). The Thr191Pro variant was comparable to the negative control, already suggesting a deficiency in catalytic activity (Fig. 4A, lane 4). When incubated with a CPD-containing template, the reticulocyte extract was not capable of performing damage bypass and elongating the primer (Fig. 4A, lane 5) resulting in the absence of any longer (> 16 bp) product. TLS activity, on the other hand, might be clearly seen when WT Pol η was expressed in the TnT system, where the polymerase was able to extend the primer to completion (Fig. 4A, lane 6). The Thr191Pro substitution renders the polymerase incompetent for bypassing the CPD and incapable of elongating the primer, in a manner again similar to the EV control (Fig. 4A, lane 7).

The primer extension assay can minimally assess the polymerase catalytic activity but cannot be considered a substitute for *in vivo* TLS analysis in cells. In order to obtain further insight into the relevance of the Thr191Pro substitution, we complemented a Pol η deficient cell line (XP30RO) with either WT or Thr191Pro Pol η , both tagged with eGFP, to assess damage bypass and UV sensitivity. In the first case, cells were irradiated with 10 J/m²

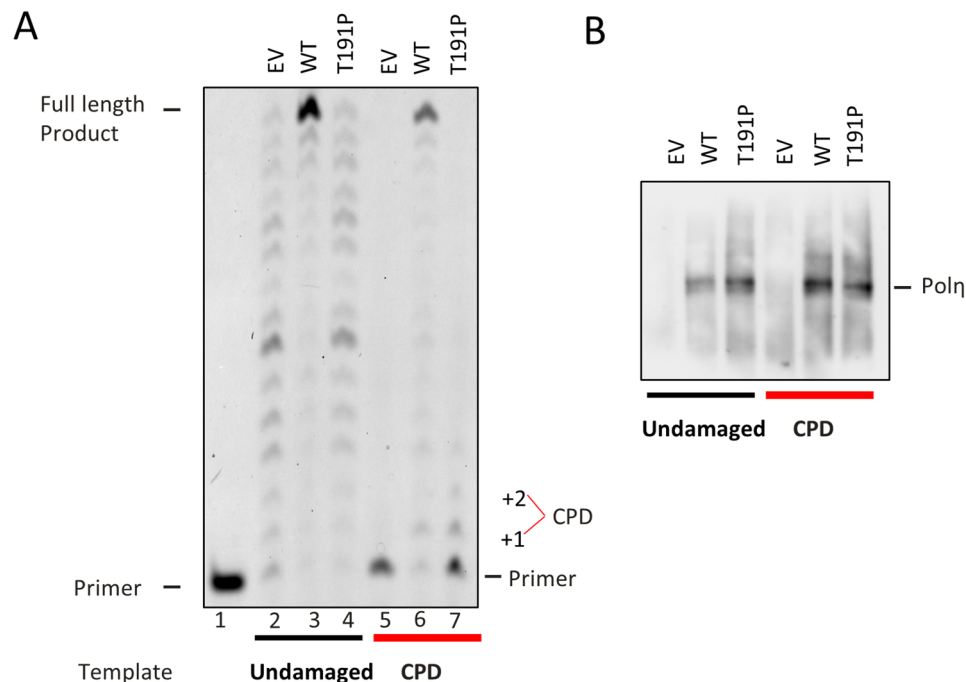


Figure 4. In vitro primer extension assay. **(A)** In vitro transcribed and translated Pol η , either wild-type (WT) or T191P, was used to extend an undamaged or a CPD containing template. EV indicates the reticulocyte extract incubated with the Empty Vector. **(B)** Western Blot quantitation of Pol η present in the assay.

and then incubated for 24 h before analyzing their cell cycle distribution by measuring their DNA content via flow cytometry. All three stable cell lines showed comparable cell cycle profiles in undamaged conditions (Fig. 5, left panels), with most of the cells having a peak at 2c DNA content. After UV, Pol η deficient cells (XP30RO) could not bypass the damage and arrested in the early stages of S phase. This cell cycle block resulted in a single broad 2c peak (Fig. 5, upper right panel). On the other hand, WT-complemented cells could bypass the damage and progress, albeit slowly, showing an increase in the number of cells in mid to late S phase or even G2 (Fig. 5, middle right panel) with 4c DNA content. As expected from the primer assay result, the Thr191Pro variant behaved essentially as the Pol η deficient cell line, indicating its inability to sustain DNA replication in the presence of DNA damage (Fig. 5, lower right panel).

Finally, UV survival assays were carried in the same cell lines. After plating, the cells were exposed to increasing amounts of UV irradiation and incubated in either the absence or the presence of caffeine (Fig. 6A,B). Pol η deficient cells show moderate sensitivity to UV (Fig. 6B, compare solid blue and purple lines), that was enhanced by the addition of low doses of caffeine (Fig. 6B, compare dashed blue and purple lines). These results are consistent with the known effects of caffeine on sensitivity to UV-C specifically in this genetic background. In fact, the increased UV sensitivity in the presence of caffeine has been used in the clinic as a diagnostic marker for many years. The cells complemented with WT Pol η became resistant to UV-C both in the presence and the absence of caffeine (Fig. 6B, solid and dashed blue lines), whereas the cells complemented with the Thr191Pro variant were even more sensitive to UV irradiation than the parental cells (Fig. 6B, solid and dashed green lines).

Discussion

DNA polymerase η is a crucial enzyme that allows replication of damaged DNA. Its relevance is exemplified in XPV patients where this polymerase is not functional. Most of the reported mutations are nonsense and occur in the catalytic domain leading to loss of protein function. With our work, we have extensively characterized the previously reported Pol η Thr191Pro variant showing that it cannot sustain damage bypass in vitro and impairs S phase progression after UV irradiation in vivo. Finally, the Pol η Thr191Pro cannot rescue the sensitivity to UV-C of XPV deficient cells indicating that this allele could be upgraded from a variant of uncertain significance to a likely pathogenic *mutant* according to ACMG guidelines, and as such providing evidence for XPV causality.

Only a small percentage of reported variants are missense, none of which, to this date, has been characterized functionally on a molecular level, thus they are still classified as being of uncertain significance in most databases.

The following overview of naturally occurring *POLH* missense variants attests to that, addressing the structural basis of their putative pathogenicity where predictable. These variants have been reported in the literature with varying phenotypic assessment and different extents of analysis. However, the common approach of using patient-derived cells precludes the criterion ‘strong evidence of pathogenicity’ (PS3) according to ACMG guidelines (Supplementary Table).

The Arg93Pro variant leads to decreased survival in response to UV and caffeine, suggesting abrogation of the UV lesion bypass. This is likely due to the loss of the arginine interaction with the template strand phosphate at

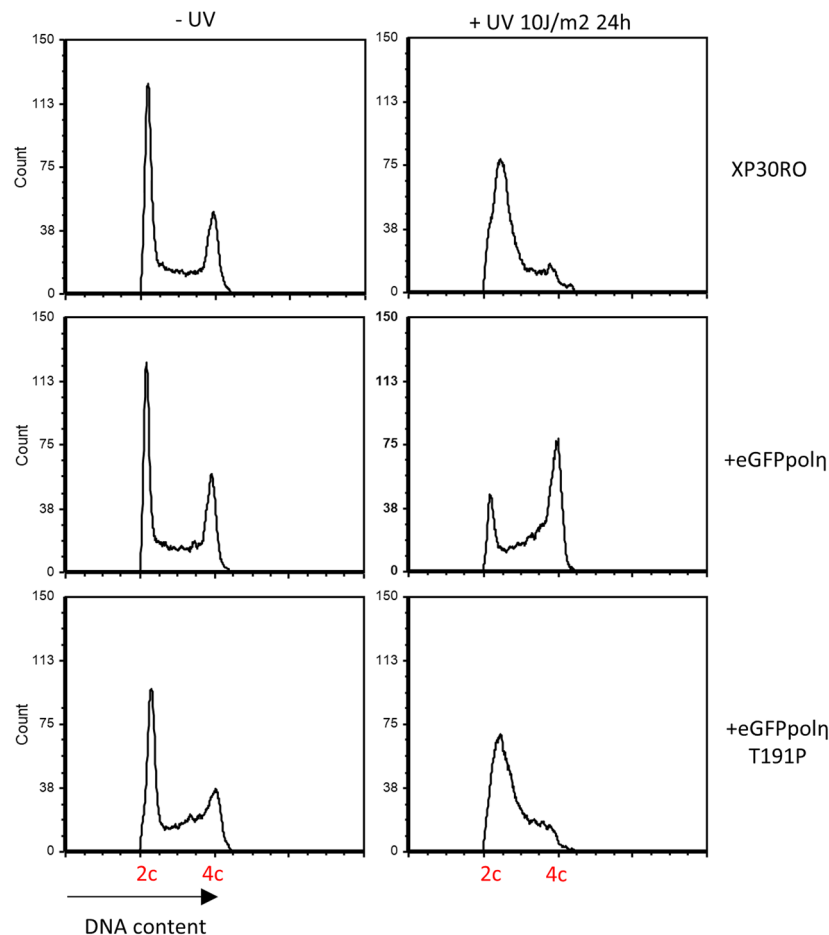


Figure 5. In vivo cell cycle analysis after UV irradiation. Stable cell lines expressing either WT or T191P eGFP-Pol η and Pol η -deficient XP30RO cells were mock treated or irradiated with 10 J/m² of UV-C and incubated for 24 h. After fixation, the cells were stained with the intercalating agent Propidium Iodide and their DNA content was measured by flow cytometry.

the – 2 position, as well as the loss of interaction between the finger and little finger domains, thus undermining the molecular splint that maintains the template strand in the normal B-form in the presence of the UV lesion. Further, the proline is expected to introduce a kink in the alpha helix¹⁴. Two other arginine missense variants, Arg111His and Arg361Ser, located in the proximity of Arg93, are expected to be analogously damaging to DNA template binding. However, no functional analysis has been done for these two variants. Patients harboring the Arg93Pro variant showed BCC, SCC, and melanoma¹⁴. Tumoral lesions in patients with Arg111His and Arg-361Ser variants were present but not characterized¹⁵.

Missense variants Gly263Val and Val266Asp, located in the thumb domain, showed no TLS in XPV cell extracts or decreased cell survival after exposure to UV and caffeine. Experiments were done in patient-derived cell lines, thus they do not fulfill functional assay criteria^{11,14,15}. Either variant is predicted to result in a less stable protein, but with less severe structure–function defect than Arg93Pro. Tumoral lesions in the respective patients were also present but not characterized.

A palm-domain located Thr122Pro variant was described in the context of compound heterozygosity with a frameshift (His407fsSer442) mutation. XPV but no skin tumors were described for this variant¹⁵. Another compound heterozygous patient with 24 melanomas and numerous carcinomas had a Gly295Arg variant on one allele, and a Pro576Argfs*3 mutation on another, resulting in truncation after the catalytic core¹⁴. The long arginine sidechain is likely to result in steric hindrance, thus destabilizing and potentially unfolding the thumb domain.

Three homozygous missense variants, recently identified in XPV patients, are located in the palm (Leu11Pro and Thr191Pro) and little finger (Cys321Phe) domains¹². The Thr191Pro variant was the only one associated with skin tumors, namely SCC, and is the same missense variant found in our patient. All three variants were reported as of uncertain significance (VUS) in the absence of functional data.

An XPV cell line with a naturally occurring homozygous Ala117Pro missense variant showed slightly decreased unscheduled DNA synthesis and increased UV sensitivity in the presence of caffeine¹⁶. Similar results were found for an XPV cell line with compound heterozygous variants (Lys535Glu, Lys589Thr)¹⁷. Another compound heterozygous variant was described with a missense variant on one allele (Lys220Glu) and a frameshift (Ser51Alafs*54) on the other. A translesion synthesis assay was reported to be normal in this cell line, as well as in

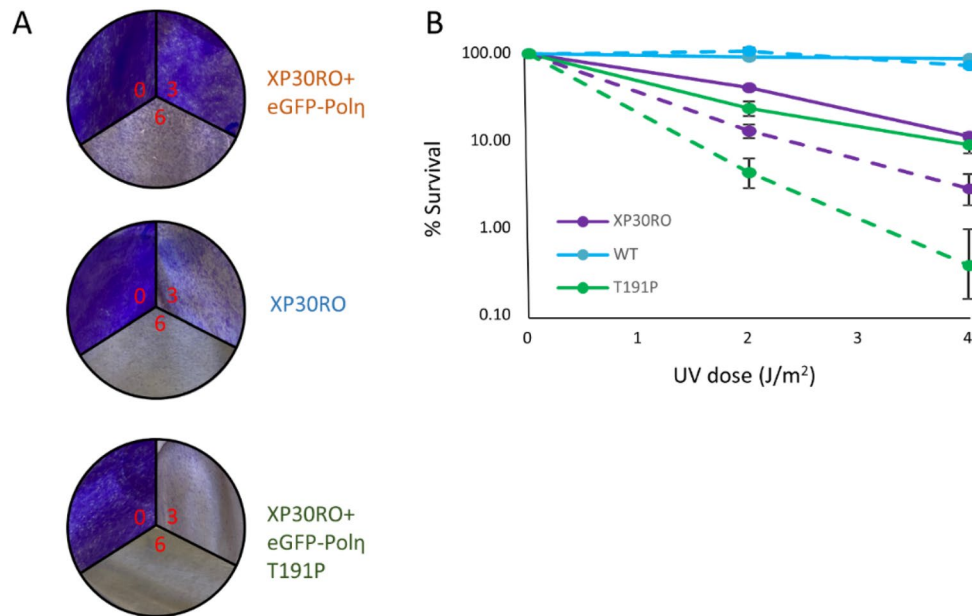


Figure 6. Cell Survival after UV irradiation. **(A)** Composite of representative images of a cell survival assay after increasing doses of UV-C (in red, J/m²) following crystal violet staining. The cells lines stably express either WT or T191P eGFP-Pol η in a pol η deficient background (XP30RO). **(B)** Quantitation of cell survival assays of the same cell lines after crystal violet staining in the absence (solid lines) or in the presence of 75 μ g/ml caffeine (dashed lines).

another with a homozygous Trp174Cys variant¹⁸. The patients from whom the cell lines were derived developed melanomas in addition to XPV.

It is interesting to note that one missense variant (Met595Val) located in the C-terminal region was not associated with XPV, but rather with melanoma and melanoma-associated carcinomas¹⁹. There are no functional data available for this variant, but one may speculate that it may be less damaging compared to XPV-associated variants, given the relatively conservative substitution away from the catalytic domain. Indeed, this is an evident example where functional analysis is of utmost importance to determine pathogenicity and an eventual predisposition to non-XPV melanoma.

Another interesting variant (Thr692Ala) was present in an allele harboring a second variant at the stop codon, both at the homozygous state, with the result being a longer (721 aa) than normal (713 aa) protein²⁰. Translesion synthesis and UV sensitivity were only slightly affected. The XPV phenotype, which showed no skin tumors, is thought to be due to proteasomal degradation of the exposed UBZ domain. Indeed, the known proteasome inhibitor, bortezomib, restored Pol η levels in a cell line stably expressing the longer protein, thus bearing therapeutic potential.

As evident from the above overview, the large majority of naturally occurring missense variants is found in the catalytic domain; only a few were present in the C-terminal of the polymerase. None of the four residues (Cys635, Cys638, His650, His654) that coordinate zinc in the ubiquitin-binding zinc finger (UBZ) domain, or any other UBZ or PCNA-interacting residue, has been found to naturally occur in patients.

To the best of our knowledge, our work describes the first functional analysis of a *POLH* missense variant shown to be catalytically defective in vitro and in vivo, thus confirming XPV causality. While the results are not surprising, based on clinical phenotype and structure–function predictions, it is important to note that without such functional analysis, the Thr191Pro will have otherwise remained VUS. Our data thus contribute to expanding the body of knowledge on Pol η and pave the way for characterization of future missense variants, establishing a robust and reliable set of molecular tests that could be quickly implemented to assess variant significance. It will also be interesting to perform functional analysis in variants not associated with XPV, such as Met595Val, or the uncharacterized Thr692Ala variant when present alone and not in the context of a longer protein²¹.

From a clinical perspective, our results enable clear genetic counseling to our patient and her descendants. Further, Pol η plays a role in acquired drug resistance through its bypass of lesions induced by platinum-based chemotherapy, and it is a pharmacological target in current major research efforts³. Gaining functional insight into critical Pol η residues is therefore key to developing small molecule inhibitors for cancer therapeutics.

Material and methods

Exome sequencing

Written informed consent was obtained from the patient prior to molecular studies. All methods were carried out in accordance with relevant guidelines and regulations. Whole-exome sequencing was performed on DNA extracted from venous blood, using the Twist Human Core Exome capture kit (Illumina NextSeq500

sequencer), followed by targeted analysis of a 19-gene panel (XP, trichothiodystrophy, or Cockayne syndrome). Reads mapping and variant calling were performed using BWA 0.7.13, Picard 2.9.0 and GATK HaplotypeCaller 3.7 and annotated with annovar 2017-07-17 and UCSC RefSeq (refGene) downloaded on 2018-08-10. Variants were searched for in various databases including Genome Aggregation Database, ClinVar, Leiden Open Variation Database and Human Gene Mutation Database. Written informed consent for publication of clinical and molecular details was obtained from the patient, available on request. The patient was not part of any human experimental study protocol. The *POLH* T191P variant has been deposited in ClinVar under the accession number SCV004218544.

Cell culture

All the experiments have been carried out with XP30RO (XP-V, also designated GM3617), transformed with SV40 T antigen, carrying a homozygous deletion in the *POLH* gene, resulting in a truncated protein of 42 amino acids. The absence of Pol η expression is regularly checked by western blot and the cells are routinely tested for mycoplasma contamination. XP30RO stably expressing Thr191Pro was created as described previously¹³. All the cells were cultured in Dulbecco's modified Eagle's medium containing 10% Fetal Bovine Serum.

UV survival assay

Cell lines expressing different eGFP Pol η constructs were plated in triplicate after cell sorting on a Bio-Rad S3e cell sorter. The following day, the cells were washed with PBS, mock treated or irradiated with UV-C (2 and 4 J/m²) and incubated in either DMEM or DMEM with 75 μ g/ml caffeine. After 72 h the cells were fixed and stained with crystal violet (0.5% Crystal violet in 20% Methanol) for 20 min at RT. After air-drying the plates, the cells were incubated for 20 min at room temperature with destain solution (0.1 M Sodium Citrate pH 4.2 in 25% Ethanol) and the absorbance (@595 nm) of each samples was analysed with a GloMax[®] Discover Microplate reader.

Primer extension assay

Primer extension assay was performed as previously described¹³. In brief, plasmids encoding Pol η -6His (WT and T191P) were transcribed and translated (TnT, Promega) in vitro in rabbit reticulocyte lysates. Pol η protein levels were quantified by western blot analysis and equimolar amounts were used in the primer extension assays. A 5' FAM-labeled 16mer (5'-CACTGACTGTATGATG-3') was annealed with a template 30mer primer (5'-CTC GTCAGCATC[cissyn-TT]CATCATAACAGTCAGTG-3') containing a thymidine dimer (TT) at position + 13 (TriLink Biotechnologies) or the undamaged control.

Extension reactions were performed in 10 μ l of replication buffer (40 mM Tris-Cl pH 8, 5 mM MgCl₂, 10 mM DTT, 0.25 mg/ml acetylated BSA, 60 mM KCl, 2.5% glycerol) at 37°C for 15 min before being stopped with of 2 \times loading buffer, (98% formamide, 10 mM EDTA pH 8, 0.025% xylene cyanol and 0.025% bromophenol blue). Boiled samples (95°C for 5 min) were then run on a 15% acrylamide-7 M urea gel and then scanned on a Typhoon TRIO imager (GE HealthCare). Western blots to assess Pol η levels were carried out as previously described²². Since the blots were used only for assessing Pol η , nitrocellulose membranes were cut in the range from 135 to 50 KDa, according to the prestained molecular marker, before incubation with the antibodies (α Pol η mAb #13848 Cell Signalling, HRP Goat Anti-Rabbit IgG 111-035-003 Jackson Immunoresearch). Uncropped images are presented in the supplementary files.

Cell cycle analysis

Cell cycle analysis was performed as in²². Briefly, the cells, either mock treated or irradiated with 10 J/m² of UV-C, were incubated for 24 h before fixation in 1 ml of 70% cold ethanol for 4 h. After centrifugation the cells were resuspended in FACS Buffer (PBS, 0.1% Tween 20, 50 μ g/ml Propidium Iodide, 5 μ g/ml RNase A) and incubated at 37 °C for 15 min to allow for RNA removal. Finally, the cells were acquired on a Bio-Rad S3e cell sorter and the data was analyzed with FCS Express (De Novo software).

Data availability

All data generated or analysed during this study are included in this published article.

Received: 19 November 2023; Accepted: 31 December 2023

Published online: 11 January 2024

References

- Jung, E. G. New form of molecular defect in xeroderma pigmentosum. *Nature* **228**, 361–362. <https://doi.org/10.1038/228361a0> (1970).
- Masutani, C. *et al.* The XPV (xeroderma pigmentosum variant) gene encodes human DNA polymerase η . *Nature* **399**, 700–704. <https://doi.org/10.1038/21447> (1999).
- Saha, P. *et al.* DNA polymerase η : A potential pharmacological target for cancer therapy. *J. Cell. Physiol.* **236**, 4106–4120. <https://doi.org/10.1002/jcp.30155> (2021).
- Tomas-Roca, L. *et al.* De novo mutations in PLXND1 and REV3L cause Mobius syndrome. *Nat. Commun.* **6**, 7199. <https://doi.org/10.1038/ncomms8199> (2015).
- Halas, A. *et al.* Developmental delay with hypotrophy associated with homozygous functionally relevant REV3L variant. *J. Mol. Med.* **99**, 415–423. <https://doi.org/10.1007/s00109-020-02033-3> (2021).
- Kannouche, P. L., Wing, J. & Lehmann, A. R. Interaction of human DNA polymerase η with monoubiquitinated PCNA: A possible mechanism for the polymerase switch in response to DNA damage. *Mol. Cell* **14**, 491–500. [https://doi.org/10.1016/s1097-2765\(04\)00259-x](https://doi.org/10.1016/s1097-2765(04)00259-x) (2004).
- Trincao, J. *et al.* Structure of the catalytic core of *S. cerevisiae* DNA polymerase η : Implications for translesion DNA synthesis. *Mol. Cell* **8**, 417–426. [https://doi.org/10.1016/s1097-2765\(01\)00306-9](https://doi.org/10.1016/s1097-2765(01)00306-9) (2001).

8. Ohashi, E. *et al.* Interaction of hREV1 with three human Y-family DNA polymerases. *Genes Cells* **9**, 523–531. <https://doi.org/10.1111/j.1356-9597.2004.00747.x> (2004).
9. Baldeck, N. *et al.* FF483-484 motif of human Poleta mediates its interaction with the POLD2 subunit of Poldelta and contributes to DNA damage tolerance. *Nucleic Acids Res.* **43**, 2116–2125. <https://doi.org/10.1093/nar/gkv076> (2015).
10. Biertumpfel, C. *et al.* Structure and mechanism of human DNA polymerase eta. *Nature* **465**, 1044–1048. <https://doi.org/10.1038/nature09196> (2010).
11. Richards, S. *et al.* Standards and guidelines for the interpretation of sequence variants: A joint consensus recommendation of the American College of Medical Genetics and Genomics and the Association for Molecular Pathology. *Genet. Med.* **17**, 405–424. <https://doi.org/10.1038/gim.2015.30> (2015).
12. Santiago, K. M. *et al.* Comprehensive germline mutation analysis and clinical profile in a large cohort of Brazilian xeroderma pigmentosum patients. *J. Eur. Acad. Dermatol. Venereol.* **34**, 2392–2401. <https://doi.org/10.1111/jdv.16405> (2020).
13. Bertolotti, F. *et al.* Phosphorylation regulates human poleta stability and damage bypass throughout the cell cycle. *Nucleic Acids Res.* **45**, 9441–9454. <https://doi.org/10.1093/nar/gkx619> (2017).
14. Opletalova, K. *et al.* Correlation of phenotype/genotype in a cohort of 23 xeroderma pigmentosum-variant patients reveals 12 new disease-causing POLH mutations. *Hum. Mutat.* **35**, 117–128. <https://doi.org/10.1002/humu.22462> (2014).
15. Broughton, B. C. *et al.* Molecular analysis of mutations in DNA polymerase eta in xeroderma pigmentosum-variant patients. *Proc. Natl. Acad. Sci. USA* **99**, 815–820. <https://doi.org/10.1073/pnas.022473899> (2002).
16. Tanioka, M. *et al.* Molecular analysis of DNA polymerase eta gene in Japanese patients diagnosed as xeroderma pigmentosum variant type. *J. Investig. Dermatol.* **127**, 1745–1751. <https://doi.org/10.1038/sj.jid.5700759> (2007).
17. Itoh, T. *et al.* Xeroderma pigmentosum variant heterozygotes show reduced levels of recovery of replicative DNA synthesis in the presence of caffeine after ultraviolet irradiation. *J. Investig. Dermatol.* **115**, 981–985. <https://doi.org/10.1046/j.1523-1747.2000.00154.x> (2000).
18. Inui, H. *et al.* Xeroderma pigmentosum-variant patients from America, Europe, and Asia. *J. Investig. Dermatol.* **128**, 2055–2068. <https://doi.org/10.1038/jid.2008.48> (2008).
19. Di Lucca, J. *et al.* Variants of the xeroderma pigmentosum variant gene (POLH) are associated with melanoma risk. *Eur. J. Cancer* **45**, 3228–3236. <https://doi.org/10.1016/j.ejca.2009.04.034> (2009).
20. Ahmed-Seghir, S. *et al.* Aberrant C-terminal domain of polymerase eta targets the functional enzyme to the proteosomal degradation pathway. *DNA Repair* **29**, 154–165. <https://doi.org/10.1016/j.dnarep.2015.02.017> (2015).
21. Jalkh, N. *et al.* Next-generation sequencing in familial breast cancer patients from Lebanon. *BMC Med. Genom.* **10**, 8. <https://doi.org/10.1186/s12920-017-0244-7> (2017).
22. Cipolla, L. *et al.* UBR5 interacts with the replication fork and protects DNA replication from DNA polymerase eta toxicity. *Nucleic Acids Res.* **47**, 11268–11283. <https://doi.org/10.1093/nar/gkz824> (2019).
23. Feltes, B. C. & Menck, C. F. M. Current state of knowledge of human DNA polymerase eta protein structure and disease-causing mutations. *Mutat. Res. Rev. Mutat. Res.* **790**, 108436. <https://doi.org/10.1016/j.mrrrev.2022.108436> (2022).

Acknowledgements

We would like to thank all the members of the lab for helpful discussion and feedback on the manuscript. We would also like to thank Elisa Mentegari for the help in performing the primer extension assay. We thank Prof. Marc Abramowicz (Division of Medical Genetics, Geneva) for support.

Author contributions

Conceptualization, O.Z. and S.S.; Methodology, O.Z. and S.S.; Investigation R.R., O.Z., C.M., T.N., G.V., G.F. and L.C.; Writing, review and editing, O.Z., T.D.H., and S.S.; Funding Acquisition: T.D.H. and S.S.

Funding

Associazione Italiana per la Ricerca sul Cancro Investigator Grant [24316 to S.S.]; MUR PRIN 2017 [2017KSZZJW to S.S.], MUR/PNRR Next Generation EU PRIN 2022 [2022JA8JY5 to S.S.], NUTRAGE [CNR project FOE-2021 DBA.AD005.225 to S.S.] and Swiss National Science Foundation [Project 182487 to T.D.H.].

Competing interests

The authors declare no competing interests.

Additional information

Supplementary Information The online version contains supplementary material available at <https://doi.org/10.1038/s41598-023-51120-1>.

Correspondence and requests for materials should be addressed to O.Z. or S.S.

Reprints and permissions information is available at www.nature.com/reprints.

Publisher's note Springer Nature remains neutral with regard to jurisdictional claims in published maps and institutional affiliations.



Open Access This article is licensed under a Creative Commons Attribution 4.0 International License, which permits use, sharing, adaptation, distribution and reproduction in any medium or format, as long as you give appropriate credit to the original author(s) and the source, provide a link to the Creative Commons licence, and indicate if changes were made. The images or other third party material in this article are included in the article's Creative Commons licence, unless indicated otherwise in a credit line to the material. If material is not included in the article's Creative Commons licence and your intended use is not permitted by statutory regulation or exceeds the permitted use, you will need to obtain permission directly from the copyright holder. To view a copy of this licence, visit <http://creativecommons.org/licenses/by/4.0/>.

© The Author(s) 2024